Analyst

COMMUNICATION

View Article Online
View Journal | View Issue

Cite this: *Analyst*, 2015, **140**, 2613

Received 8th December 2014,
Accepted 16th February 2015

DOI: 10.1039/c4an02253j

www.rsc.org/analyst

Solvatochromic sensor array for the identification of common organic solvents†

Jacqueline M. Rankin,‡ Qifan Zhang,‡ Maria K. LaGasse, Yinan Zhang, Jon R. Askim and Kenneth S. Suslick*

A cross-reactive colorimetric sensor array composed of solvatochromic dyes in semi-liquid matrices was used to successfully discriminate among eleven common solvents. The multidimensional array response is attributed to both chemical (*i.e.*, analyte–dye interactions) and physical (*i.e.*, spot blooming and refractive index alteration) changes in the sensor spot.

Colorimetric sensor arrays use multiple chemically responsive dyes to generate a pattern of color changes that represent a composite, olfactory-like response unique to a given odorant: they are essentially "optoelectronic noses".[1–4] The color changes can be quantitatively measured through digital imaging of the array by comparing images before and during exposure (*e.g.*, with a flatbed scanner or digital camera). We have developed colorimetric arrays to differentiate on the basis of chemical reactivity both single component analytes (including toxic industrial chemicals (TICs), VOCs, explosives)[5–9] and complex mixtures (*e.g.*, coffees,[10] sodas,[11] beers,[12] and microorganisms[13,14]). The colors of utilized dyes are affected by intermolecular interactions between analyte and dye, including Brönsted and Lewis acid–base, hydrogen bonding, dipolar, and π–π interactions. In general, these arrays were optimized for analytes with significant chemical reactivity (*e.g.*, TICs). The use of a colorimetric sensor array to differentiate among poorly-reactive analytes (*e.g.*, common laboratory solvents) below their saturation concentration has proved challenging.

Solvatochromic compounds change color in response to a change in polarity of the local environment, an effect caused by a polarity difference between the chromophore's ground and excited state,[15,16] and are, therefore, commonly used to probe solvent polarity.[15–20] Solvatochromic dyes can be broadly classified as exhibiting either positive solvatochromism, where the ground state is less polar than the excited state, or negative solvatochromism, where the ground state is more polar than the excited state.[15] Historically, these color-changing dyes have been studied in liquid phase and characterized using UV-Vis absorption spectroscopy; however, some recent work has used individual solvatochromic dyes in solids (*e.g.*, films of dyes entrapped in porous, semi-liquid, or polymer matrices).[21–25] Prior colorimetric sensor arrays produced from our lab have included only one or two solvatochromic sensor spots, but the response of an array of solvatochromic dyes in the solid-state has not been previously examined.

We report here a colorimetric sensor array that utilizes solvatochromic dyes in semi-liquid matrices to differentiate eleven common organic solvents. Importantly, the solvatochromic dyes serve a dual function: (1) to change color with a change in local polarity and (2) to facilitate the measurement of physical changes in their matrix caused by solvent sorption. The array response can be monitored using an ordinary flatbed scanner, providing a convenient means of detection.[4,8,26] We are also able to decouple these two types of response through a comparison of the RGB (red, green, and blue) reflectance with full spectral reflectometry data of representative sensor spots. This work demonstrates a novel method to discriminate among analytes that have limited chemical reactivity and also provides a cautionary tale for colorimetric sensing in general: observed changes in RGB values may reflect physical rather than chemical interactions between the sensor and the analyte, especially at high analyte concentrations.

Colorimetric sensor arrays were prepared as described elsewhere;[1] briefly, solvatochromic dyes were dissolved in dilute solutions of a volatile solvent containing both the dye and a highly viscous liquid and then printed on porous polypropylene membranes using a robotic pin printer. After evaporation, the dyes were held in a semi-fluid state dissolved in the viscous matrix supported by the membrane. A summarized list of dyes is shown in Table S1.† Seven commonly used solvatochromic compounds (four positive solvatochromic and three negative solvatochromic dyes[19,20,27,28]) were chosen.

Because solvatochromic compounds are sensitive to the polarity of the local environment, the starting color of a spot

Department of Chemistry, University of Illinois at Urbana-Champaign, 600 South Mathews Avenue, Urbana, Illinois 61801, USA. E-mail: ksuslick@illinois.edu

†Electronic supplementary information (ESI) available. See DOI: 10.1039/c4an02253j

‡Authors contributed equally.

containing a solvatochromic dye is highly dependent on the matrix (*i.e.*, the dye's local environment). In order to maximize interaction between analytes and a solvatochromic dye (or for that matter, any indicator), one must minimize interactions between the ground state of the dye and its surrounding matrix. The matrix, therefore, must be chosen carefully; a poorly matched matrix will diminish spot response. In choosing an appropriate matrix, the inherent chemical properties of the dye (*e.g.*, ground state polarity, potential for hydrogen bonding)[15,29] must be considered.

Generally, positive solvatochromic dyes were dissolved in relatively polar matrices (*i.e.*, glycerol or ionic liquid) and negative solvatochromic dyes were dissolved in relatively nonpolar matrices (*i.e.*, methylsiloxanes), as listed in Table S2.† To enhance chemical diversity of the responses of the sensors, dyes were dissolved in multiple matrices, *i.e.*, polar, nonpolar, and medium polarity (*e.g.*, benzyl butyl phthalate, BBP). In addition, matrices with differing intermolecular forces (*e.g.*, H-bonding, dipole–dipole) will sorb different classes of analytes preferentially, thus affecting the response profile from each formulation. As given in Table S3,† an array of 18 sensor spots using seven solvatochromic dyes among four matrices was generated. Our use of different formulations for the matrices of the solvatochromic dyes is analogous to the use of multiple polymers of different polarities in sensor arrays.[30–33]

Even in an instance where there is no direct dye–analyte interaction, a sensor spot may still show a change in RGB values through sorptive effects. When an analyte is present at high concentration, its sorption into a semi-liquid matrix may change the properties of the matrix (*e.g.*, viscosity, refractive index). Viscosity changes may cause blooming of the spot, *i.e.*, a diffusion of the spot edge, making the spot larger but less intensely colored. Changes in the refractive index of the spot can change the intensity of light reflected from the surface.[34,35] These effects manifest as a change in color intensity (*i.e.*, a change in RGB values from digital images of the spot). Changes in RGB values, whether due to wavelength shift of the dye, blooming of the sensor spot, or alteration of the spot's refractive index, all may be useful to facilitate analyte identification and discrimination. The matrices used in this study were chosen to maximize both solvatochromic and sorptive responses.

For this work, eleven common solvents with polarities evenly distributed over a wide range of $E_T(30)$ values[19] were chosen as analytes. Table S4† lists these analytes and their $E_T(30)$ values. Arrays were exposed to flowing gas (500 sccm) containing a given analyte at 10% the saturation concentration in dry nitrogen. Images were processed according to previously described procedures;[4,7–10,14,26,36] a more detailed explanation of experimental protocols and data processing can be found in the ESI.†

Difference maps are a useful tool for qualitatively visualizing how an array changes color when exposed to a given analyte. Representative difference maps showing the unique response pattern to each analyte after 5 minutes exposure are shown in Fig. 1; responses were measured in quintuplicate on

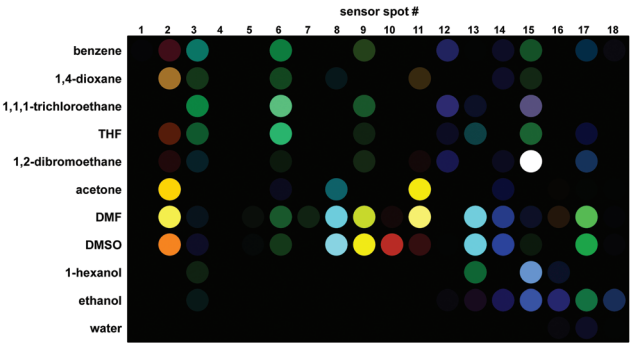

Fig. 1 Difference maps showing the colorimetric sensor array response to eleven analytes at 10% of their saturation vapor pressure after 5 min of exposure (averages of five trials each are shown). A color range of 1.5–8.5 was expanded to 8-bit color range (*i.e.*, 0–255) for visualization. A complete list of the 18 sensor spot formulations can be found in Table S3.†

separate arrays. Using the raw digital data, a hierarchical cluster analysis (HCA) was performed to quantify differentiability among analytes (Fig. 2). There is clear discrimination among all eleven solvents, showing no misclassifications for 62 trials. HCA generates a dendrogram that provides a quantitative analysis of response similarity among hierarchically-ranked clusters. Sensors with similar response patterns, as determined by the distance between individual trials in the 54 dimensional space (*i.e.*, ΔRGB values of 18 spots), will cluster together. Thus, the connectivity of an HCA diagram shows "what resembles what" and the Euclidean distance at which clusters are grouped shows "by how much."

Principal component analysis (PCA), when applied to chemical sensor arrays, gives an approximation of the dimensionality of the chemical properties space being probed by the array. Often, sensor arrays require only 1 or 2 dimensions to capture 95% or even 99% of the total variance among responses. This lack of dimensionality indicates the sensor

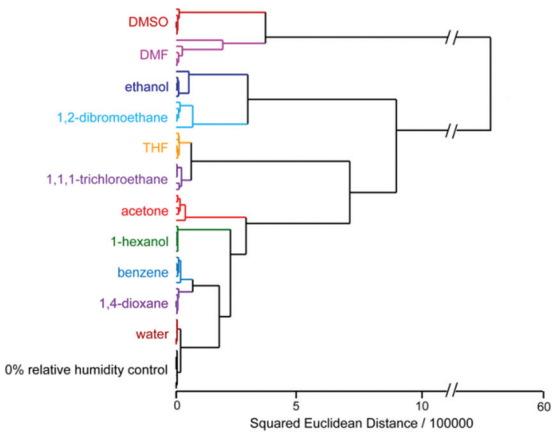

Fig. 2 Hierarchical cluster analysis of the colorimetric array response to 11 common organic solvents and the control. The 11 analytes were run in quintuplicate and the dry N_2 control was run in septuplicate. The HCA used minimum variance (*i.e.*, ward's method) for clustering. No misclassifications were observed among the 62 trials.

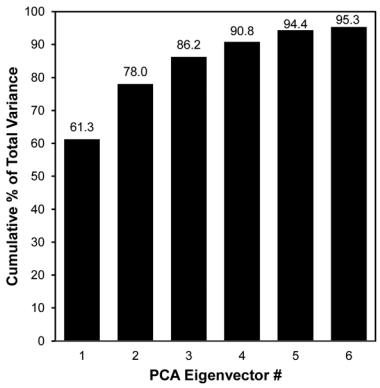

Fig. 3 Scree plot of the principal components from PCA from 11 analytes and a N_2 control. Six dimensions are required to define 95% of the total variance.

array is actually probing only one or two chemical parameters with hydrophobicity typically predominant. This means that many so-called sensor arrays in the literature may physically be arrays (*i.e.*, multiple sensors), but in fact statistically they are not truly arrays at all (*i.e.*, the responses are one-dimensional). The Scree plot (Fig. 3) shows that our solvatochromic sensor array requires a total of six dimensions to reach 95% variance and therefore probes a larger number of chemical interactions than most of the electronic nose literature. This high dimensionality is not surprising; multiple factors influence array response, including solvent polarity (*i.e.*, solvatochromism), acid–base interactions (both Brønsted and Lewis), relative stability of dye–analyte interactions *versus* dye-matrix interactions, analyte-matrix affinity (*i.e.*, partition coefficient), hydrogen bonding between dyes and analytes, and the physical properties of the matrix after analyte sorption.

To decouple the changes in RGB values caused by a wavelength shift (*i.e.*, due to analyte–dye interaction) from those caused by sorptive effects (*e.g.*, refraction index changes or spot blooming), we have analyzed the full spectral reflectometric response of two representative spots (spot #15, Reichardt's dye in BBP, and spot #3, Nile red in BBP) using a diffuse reflectance probe. Fig. 4 shows the pseudo-absorbance spectra in Kubelka–Munk (K–M)[37] units and raw images of representative sensor spots that exhibit color changes caused by either (1) a solvatochromic wavelength shift (Fig. 4a,b, spot #15 exposed to ethanol) or (2) sorptive effects (Fig. 4c,d, spot #3 exposed to benzene). When a sensor spot acts as a solvatochromic probe, a color change is observed in the raw images and a wavelength shift is seen in the absorbance spectrum. When only spot blooming or refraction effects are present, the peak wavelength is unchanged, and only a change in absorbance intensity is observed. The raw images in Fig. 4d and S3† show a blurring of the spot, especially around the edges, due to the blooming of the dye spot caused by analyte sorption.

This multidimensional array response has been further demonstrated by comparing the array response of analytes with similar polarities (*i.e.*, $E_T(30)$ values). Our solvatochromic array showed clearly differentiable responses when exposed to

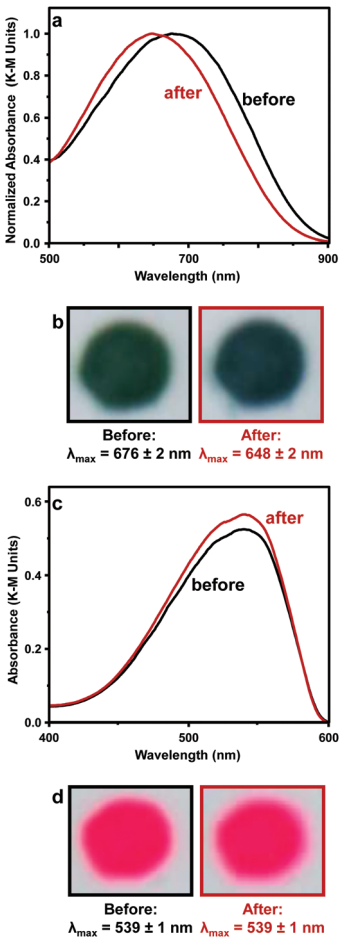

Fig. 4 (a) Diffuse reflectance spectra and (b) raw images of Reichardt's dye in BBP (Spot #15) before (black) and after (red) 5 minutes exposure to 10% saturated ethanol vapor showing the wavelength shift. (c) Diffuse reflectance spectra and (d) raw images of Nile red in BBP (Spot #3) before (black) and after (red) 5 minutes exposure to 10% saturated benzene vapor. Both spots exhibit changes in RGB values under the respective experimental conditions: in Reichardt's dye this is due mostly to solvatochromic shifts in wavelength of absorbance, but in Nile red it is due only to sorptive effects (see also Fig. S3†).

three analytes with $E_T(30)$ values of ≈40 kcal mol^{-1} (pyridine, cyclohexanone, and 2,4-dimethyl-3-pentanol) and three analytes (decane, cyclohexane, and 2-methylbutane) with $E_T(30)$ values of ≈31 kcal mol^{-1} (Fig. S1 and S2†). The difference maps showed no strong correlation between response and $E_T(30)$, and similar polarity analytes do not necessarily cluster together. These results confirm that our colorimetric array is probing more than just analyte polarity. Importantly, these arrays clearly show both chemical (*i.e.*, color changes from dye–analtye interactions) and physical (*e.g.*, dye diffusion) changes of the sensor spots when exposed to solvent vapors as shown in Fig. S3.†

At high analyte concentrations (≥10% of saturation vapor pressure), unexpected contributions to the array response come from physical, sorptive changes in the sensor spot caused by the sorption of analytes into the semi-liquid

matrices. These include both spot blooming (*i.e.*, dye diffusion) and alteration of the index of refraction (*i.e.*, changes in scattering and therefore reflectometry). This work not only describes a novel method to discriminate among common organic solvents, but also demonstrates that observed changes in RGB values can reflect physical rather than chemical interactions between the sensor and the analyte, especially at high analyte concentrations.

Conclusions

We have examined solvatochromic dye-matrix combinations printed on membranes as inexpensive, disposable colorimetric sensor arrays and demonstrated their ability to discriminate among eleven common solvents at 10% saturation concentration. Hierarchical cluster analysis shows no misclassifications among 62 trials, and PCA shows the colorimetric sensor array has high dimensionality, demonstrating the potential to discriminate among even closely related analytes. This observed high dimensionality is not surprising, as the composite array response reflects not only changes in spots' absorbance maxima (*e.g.*, from a change in local polarity), but also changes in the intensity of reflectance (*e.g.*, from spot blooming or index of refraction changes). Although these effects can be decoupled using full spectral data, care must be taken in interpreting ΔRGB values, particularly at high analyte concentrations: apparent changes in RGB values may be due both analyte–dye interactions (which will change both intensity and wavelength of light absorbance) and to changes caused by analyte sorption (which include both refractive index changes and blooming of semi-fluid spots).

Acknowledgements

This work was supported by the US NSF (CHE 1152232) and in part by the Department of Defense (JIEDDO/TSWG CB3614), the National Science Foundation Graduate Research Fellowship Program under grant no. DGE-1144245 (JMR) and a Department of Education GAANN Fellowship (MKL). JMR gratefully acknowledges fellowship support from the Robert C. and Carolyn J. Springborn Endowment.

Notes and references

1 J. R. Askim, M. Mahmoudi and K. S. Suslick, *Chem. Soc. Rev.*, 2013, **42**, 8649–8682.
2 P. Gründler, *Chemical Sensors: An Introduction for Scientists and Engineers*, Springer-Verlag Berlin Heidelberg, New York, 2007.
3 P. C. A. Jeronimo, A. N. Araujo and M. C. B. S. M. Montenegro, *Talanta*, 2007, **72**, 13–27.
4 N. A. Rakow and K. S. Suslick, *Nature*, 2000, **406**, 710–713.
5 L. Feng, C. J. Musto and K. S. Suslick, *J. Am. Chem. Soc.*, 2010, **132**, 4046–4047.
6 S. H. Lim, L. Feng, J. W. Kemling, C. J. Musto and K. S. Suslick, *Nat. Chem.*, 2009, **1**, 562–567.
7 L. Feng, C. J. Musto, J. W. Kemling, S. H. Lim and K. S. Suslick, *Chem. Commun.*, 2010, **46**, 2037–2039.
8 L. A. Feng, C. J. Musto, J. W. Kemling, S. H. Lim, W. X. Zhong and K. S. Suslick, *Anal. Chem.*, 2010, **82**, 9433–9440.
9 M. C. Janzen, J. B. Ponder, D. P. Bailey, C. K. Ingison and K. S. Suslick, *Anal. Chem.*, 2006, **78**, 3591–3600.
10 B. A. Suslick, L. Feng and K. S. Suslick, *Anal. Chem.*, 2010, **82**, 2067–2073.
11 C. Zhang and K. S. Suslick, *J. Agric. Food Chem.*, 2007, **55**, 237–242.
12 C. Zhang, D. P. Bailey and K. S. Suslick, *J. Agric. Food Chem.*, 2006, **54**, 4925–4931.
13 J. R. Carey, K. S. Suslick, K. I. Hulkower, J. A. Imlay, K. R. C. Imlay, C. K. Ingison, J. B. Ponder, A. Sen and A. E. Wittrig, *J. Am. Chem. Soc.*, 2011, **133**, 7571–7576.
14 Y. Zhang, J. R. Askim, W. Zhong, P. Orlean and K. S. Suslick, *Analyst*, 2014, **139**, 1922–1928.
15 C. Reichardt and T. Welton, *Solvents and solvent effects in organic chemistry*, Wiley-VCH, Weinheim, Germany, 4th edn, 2011.
16 E. Buncel and S. Rajagopal, *Acc. Chem. Res.*, 1990, **23**, 226–231.
17 A. R. Katritzky, D. C. Fara, H. F. Yang, K. Tamm, T. Tamm and M. Karelson, *Chem. Rev.*, 2004, **104**, 175–198.
18 R. Martinez-Manez and F. Sancenon, *Chem. Rev.*, 2003, **103**, 4419–4476.
19 C. Reichardt, *Chem. Rev.*, 1994, **94**, 2319–2358.
20 V. G. Machado, R. I. Stock and C. Reichardt, *Chem. Rev.*, 2014, **114**, 10429–10475.
21 K. Ichimura, A. Funabiki and K. Aoki, *Chem. Lett.*, 2010, **39**, 586–587.
22 K. Ichimura, K. Aoki, H. Akiyama, S. Horiuchi, S. Nagano and S. Horie, *J. Mater. Chem.*, 2010, **20**, 4312–4320.
23 D. J. Macquarrie, S. J. Tavener, G. W. Gray, P. A. Heath, J. S. Rafelt, S. I. Saulzet, J. J. E. Hardy, J. H. Clark, P. Sutra, D. Brunel, F. di Renzo and F. Fajula, *New J. Chem.*, 1999, **23**, 725–731.
24 C. Rottman, G. S. Grader, Y. DeHazan and D. Avnir, *Langmuir*, 1996, **12**, 5505–5508.
25 S. J. Tavener, J. H. Clark, G. W. Gray, P. A. Heath and D. J. Macquarrie, *Chem. Commun.*, 1997, 1147–1148.
26 S. H. Lim, J. W. Kemling, L. Feng and K. S. Suslick, *Analyst*, 2009, **134**, 2453–2457.
27 S. Y. Bae and B. R. Arnold, *J. Phys. Org. Chem.*, 2004, **17**, 187–193.
28 J. F. Deye, T. A. Berger and A. G. Anderson, *Anal. Chem.*, 1990, **62**, 615–622.
29 C. N. R. Rao, S. Singh and V. P. Senthilnathan, *Chem. Soc. Rev.*, 1976, **5**, 297–316.
30 H. C. McCaig, E. Myers, N. S. Lewis and M. L. Roukes, *Nano Lett.*, 2014, **14**, 3728–3732.
31 J. L. Martínez-Hurtado, C. A. B. Davidson, J. Blyth and C. R. Lowe, *Langmuir*, 2010, **26**, 15694–15699.

32 J.-T. Zhang, L. Wang, J. Luo, A. Tikhonov, N. Kornienko and S. A. Asher, *J. Am. Chem. Soc.*, 2011, **133**, 9152–9155.
33 J. Park, W. A. Groves and E. T. Zellers, *Anal. Chem.*, 1999, **71**, 3877–3886.
34 J. F. Donnelly and N. M. Massa, *Light: Introduction to optics and photonics*, The New England Board of Higher Education, Boston, MA, 2007.
35 P. Pilla, A. Cusano, A. Cutolo, M. Giordano, G. Mensitieri, P. Rizzo, L. Sanguigno, V. Venditto and G. Guerra, *Sensors*, 2009, **9**, 9816–9857.
36 H. W. Lin and K. S. Suslick, *J. Am. Chem. Soc.*, 2010, **132**, 15519–15521.
37 B. Hapke, *Theory of reflectance and emittance spectroscopy*, Cambridge University Press, Cambridge, 2nd edn, 2012.